Exchange bias of polycrystalline Co on single-crystalline $Fe_xZn_{1-x}F_2$ thin films

Hongtao Shi,* Zhongyuan Liu, and David Lederman
Department of Physics, West Virginia University, Morgantown, West Virginia 26506-6315, USA
(Received 13 April 2005; revised manuscript received 12 September 2005; published 12 December 2005)

The exchange bias of polycrystalline Co films grown on epitaxial, 67-nm-thick single-crystalline films of (110) $Fe_xZn_{1-x}F_2$ films was measured as a function of Fe concentration. A set of samples was grown with a pure, 1.0-nm-thick FeF_2 layer at the interface, and another set was grown without the interface layer. Unlike previous measurements of *twinned* $Fe_xZn_{1-x}F_2$ films, the exchange bias of samples with the pure interface layer remained relatively constant as the Fe concentration was decreased from $x=1.0$ to 0.35. A decrease in H_E with increasing x in samples without the pure interface layer was also observed, which can be explained by a weakening of the $Fe_xZn_{1-x}F_2$/Co exchange interaction as the Fe concentration is decreased. Evidence for the creation of frozen domains in the antiferromagnet was obtained from vertical shifts in the hysteresis loops at low temperatures for samples with $x \leqslant 0.75$, which agrees with the critical concentration $x_C=0.76$ above which antiferromagnetic domains are not expected to form due to lack of percolation of nonmagnetic impurities. The large enhancement of exchange bias expected from the domain state model is not observed in these samples because of the existence of the critical concentration in $Fe_xZn_{1-x}F_2$.

DOI: 10.1103/PhysRevB.72.224417 PACS number(s): 75.70.Cn, 75.25.+z, 75.30.Gw, 75.50.Ee

I. INTRODUCTION

The phenomenon of exchange bias, characterized by the shift of the magnetic hysteresis loop of a ferromagnet (F) away from $H=0$ when the F is coupled to an antiferromagnet (AF) or a ferrimagnet, was originally discovered in Co particles whose surface was oxidized to form CoO.[1] Since then, this effect has been observed in a large number of systems, including ferrimagnetic/ferromagnetic bilayers.[2,3] Because of its applications in data storage technology, much research has been performed recently to obtain a more fundamental understanding of the effect.

Several theories have been proposed to explain the various discrepancies with a direct interface exchange coupling mechanism,[4] including the fact that polycrystalline AF's produce a nonzero exchange bias; that the magnitude of the effect is smaller than expected; and that nominally compensated AF surfaces also show an effect. Alternate theories include the formation of domain walls parallel to the surface during magnetization reversal;[5] formation of antiferromagnetic domains perpendicular to the surface during the cooldown procedure;[6–8] a combination of an effective perpendicular anisotropy and AF domain formation;[9] and proposed more recently that nonmagnetic impurities can cause the AF to form a net magnetic moment that increases the F/AF coupling (domain state model).[10,11] Experiments on $Co_xMg_{1-x}O$ and oxygen-deficient CoO thin films,[10,12] as well as on twinned $Fe_xZn_{1-x}F_2$ samples,[13] seem to support the domain state model. Monte Carlo simulations also seem to support this viewpoint, at least qualitatively, although the impurity concentration that maximizes the effect does not coincide with the observed data.[11] Another interesting observation is that the maximum enhancement in $Co_xMg_{1-x}O$ (300%) is significantly larger than in twinned $Fe_xZn_{1-x}F_2$ samples (30%).

FeF_2 is a model antiferromagnet with a tetragonal crystal structure and a single easy axis. Exchange bias using this material, originally grown twinned on MgO,[14] has led to significant discoveries, including positive exchange bias,[15] asymmetric hysteresis loops,[16] and stimulated theoretical work in the area.[17–21] Recently *single-crystalline* (110) FeF_2-based exchange bias samples were grown via molecular beam epitaxy on MgF_2.[22] The exchange bias in these samples revealed an extreme sensitivity to the cooling field direction,[22] and provided new insights into the fundamental behavior of exchange bias above the Néel temperature of the antiferromagnet.[23] The observation of these phenomena, which are not observed in twinned samples, is a result of an improved structural quality of these single-crystalline samples.

Here we present a systematic study of single-crystalline, epitaxial $Fe_xZn_{1-x}F_2$ thin films with Co overlayers. We find that the exchange bias effect is independent of x for the range between $x=1.0$ and $x=0.35$. This raises questions about the domain state model, including whether other types of structural defects, in addition to nonmagnetic impurities, are needed to enhance the exchange bias.

II. EXPERIMENTAL DETAILS

A. Sample growth and description

The samples were grown on MgF_2 (110) single crystals via molecular beam epitaxy, using the substrate temperature and other growth conditions previously used for single-crystalline FeF_2.[22] FeF_2 and ZnF_2 were codeposited from an electron beam source and a Knudsen cell source, respectively, as was previously done for $Fe_xZn_{1-x}F_2$ twinned samples grown on MgO (100).[13] The actual thickness of the samples was determined from a quantitative analysis of x-ray reflectivity data and the Fe concentration x from measurements of the (001) lattice parameter.[13]

The thickness of all antiferromagnetic layers was approximately 67 nm and the Co overlayers were polycrystalline, with a thickness of approximately 18 nm. In order to prevent oxidation, all samples were capped with a 5-nm-thick MgF_2

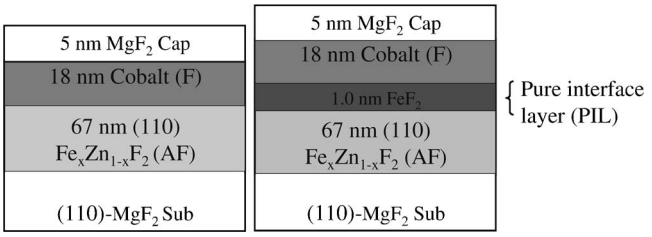

FIG. 1. Sketch of samples used in this study.

layer deposited at room temperature. The samples used for our experiments had Fe concentrations ranging between 0.3 and 1.0. Two types of samples were grown as sketched in Fig. 1: one having a 1.0 nm pure interface layer (PIL) of FeF_2, and another without the PIL, as was previously done for the $Co_xMg_{1-x}O/Co$ system[10,12] and twinned $Fe_xZn_{1-x}F_2$ samples.[13] The rationale for this was to make the AF/F exchange the same for all samples with the PIL independent of their Fe concentration. The samples without the PIL were grown to determine what other effects the PIL may have had on the exchange bias.

In order to avoid structural differences between samples having the PIL and those not having the PIL, we constructed a special sample holder where two substrates were mounted at the same time. After the growth of the AF layer, one sample was removed from the sample holder and transferred to another ultrahigh-vacuum chamber, without exposing the sample to air. The other sample was reinserted into the deposition chamber and the PIL was deposited. Afterwards, the stored sample was placed back on the sample holder, and the Co and subsequent MgF_2 capping layers were simultaneously deposited on both samples.

B. Structural characterization

The surface crystal structure was analyzed *in situ* via reflection high-energy electron diffraction (RHEED). The crystallography and interface structure was analyzed *ex situ* from x-ray diffraction and reflectivity data, obtained from a rotating anode source using Cu K_α radiation. In-plane lattice parameters were determined from the (332) Bragg reflections, which have a component of the x-ray momentum transfer vector **q** pointing in the plane of the sample.[24,25] The positions of the Bragg peaks were modeled using two Gaussians corresponding to the Cu $K_{\alpha 1}$ and $K_{\alpha 2}$ wavelengths (0.154 06 and 0.154 40 nm, respectively). Using the out-of-plane (110) lattice parameter and the (332) lattice parameter, together with the assumption of a tetragonal crystal structure, it was possible to determine the in-plane (001) *c*-axis lattice parameter from the relation

$$d_{(001)} = 2(d_{(332)}^{-2} - 9d_{(110)}^{-2})^{-1/2}, \quad (1)$$

where d_{hkl} is the interplanar distance between (hkl) planes. The Fe concentration x was determined from the *c*-axis lattice parameter using a linear interpolation between the *c*-axis lattice parameters obtained for the $x=1.0$ and 0.0 samples.[13]

ϕ scans of the (332) reflection, carried out by rotating the sample about the surface normal with the angle of incidence and detection angle set at the (332) Bragg condition, were performed to determine the in-plane crystalline symmetry.[24,25] Reflectivity data were fitted to a recursive optical model to determine the thickness of each layer, as well as the interface roughness between adjacent layers.[26]

The surfaces of the MgF_2, $Fe_xZn_{1-x}F_2$, and Co layers were imaged *in situ* using atomic force microscopy (AFM). This was accomplished by transferring the sample after the growth of each layer to a commercial scanning probe microscope with an AFM needle sensor, without exposing the sample to the atmosphere, through a transfer chamber with a base pressure of 1×10^{-9} Torr. This permitted us to compare the interface roughness of all samples under the same conditions.

C. Magnetization measurements

The exchange bias was measured in a superconducting quantum interference device (SQUID) magnetometer after field-cooling the sample from $T=100$ to 5 K. Note that $T_N \approx 78$ K for pure FeF_2 so all samples were cooled from above their T_N. Both the cooling field H_{CF} and the measuring field H were applied parallel to the $Fe_xZn_{1-x}F_2$ [001] direction, that is, in the plane of the sample and parallel to the *c* axis. The exchange bias was measured as a function of temperature, determined from the shift of the center of the hysteresis loop away from $H=0$.

III. RESULTS AND DISCUSSION

A. Structure

The RHEED patterns obtained immediately after growth of the $Fe_xZn_{1-x}F_2$ layer were streaky, as shown in Fig. 2, with no discernible transmission spots. This indicated that the surface was reasonably flat. All samples had similar patterns, indicating that the surface roughness was not highly dependent on the Fe concentration. The patterns were twofold symmetric when the samples were rotated about their surface normal, indicating that the samples were indeed epitaxial and untwinned.

The x-ray reflectivity data indicated that the interface roughness at the $Fe_xZn_{1-x}F_2/Co$ interface was approximately 0.5–0.8 nm for all samples, as shown in Fig. 3. The roughness at the top of the Co layer was approximately 0.8–1.0 nm. Similar results were obtained from the root-mean-squared surface roughness of AFM images.

The wide-angle x-ray diffraction data indicate that the antiferromagnetic layers are highly crystalline along the [110] growth direction, with a structural coherence length ξ estimated from Scherrer's equation[27] [$\xi=0.9\lambda/\cos(\theta)\Delta(2\theta)$, where θ is the Bragg diffraction angle of the (220) peak, $\Delta(2\theta)$ the full width at half maximum of the Bragg peak, and $\lambda=0.154\,06$ nm is the x-ray wavelength], of between 24 and 45 nm. The in-plane coherence was between 6 and 12 nm. The lattice parameters and structural coherence lengths are summarized in Table I. Clearly the crystalline coherence of the samples degraded slightly as the Fe concentration decreased, especially in the in-plane direction. This may be due to a non-zero correlation in the distribution of the Zn impu-

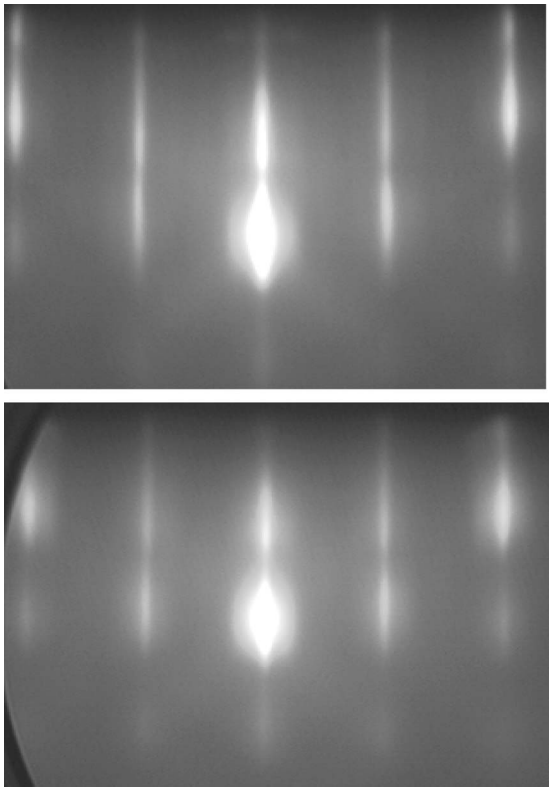

FIG. 2. RHEED patterns obtained from the surface of the $Fe_xZn_{1-x}F_2$ surface with the electron beam along the $[1\bar{1}0]$ direction for $x=1.0$ (top) and 0.36 (bottom).

rities, evidenced by the correlation length of the pure ZnF_2 ($x=0$) sample, which is larger than those of the dilute samples with $x<0.85$. ϕ scans of the sample revealed a twofold symmetry of the (332) peak. In addition, two (402) peaks were also visible, at 90° from the (332) peaks, since the diffraction condition is very similar to that of the (332) peak, as shown in Fig. 4. However, the intensity of the (402) peaks was small because the detector and sample position were not exactly optimized for the (402) diffraction condition. This was verified by optimizing for the (402) peaks and redoing the scans, in which case the intensity relation between the two types of peaks was reversed. The purported twofold symmetry was confirmed by the RHEED measurements mentioned above.

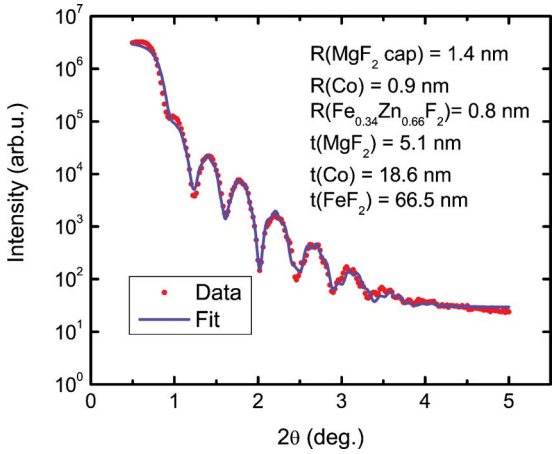

FIG. 3. (Color online) Specular x-ray reflectivity for the $x=0.36$ sample, without PIL, with fit to optical model. R represents interface roughness parameters and t layer thicknesses.

TABLE I. Structural parameters obtained from the x-ray diffraction. ξ_{hkl} are the structural coherence lengths along $[hkl]$ crystallographic directions and d_{hkl} interplanar distances for (hkl) planes. The Fe concentration x was determined from d_{001} by interpolating between the $x=1.0$ and 0.0 values. Uncertainties for x are $\sim\pm0.02$ (except for the $x=1.0$ and 0.0 pure samples) and for d are $\sim\pm0.0002$ nm.

x	d_{110} (nm)	ξ_{110} (nm)	d_{001} (nm)	ξ_{001} (nm)
1.00	0.3333	45.4	0.3292	11.0
0.97	0.3331	28.8	0.3288	12.1
0.85	0.3328	34.5	0.3267	10.1
0.77	0.3327	26.5	0.3254	7.8
0.65	0.3329	25.3	0.3233	7.3
0.36	0.3332	24.6	0.3185	5.8
0.00	0.3330	31.0	0.3125	8.7

The important conclusions from the structural studies are that (1) all samples had similar interface roughness parameters, and (2) the $Fe_xZn_{1-x}F_2$ layers of all samples were epitaxial. Hence, differences in the magnetic properties observed among the samples are likely to be due to changes in Fe concentration.

B. Magnetic hysteresis loops

Representative hysteresis loops obtained at $T=5$ K after cooling in a field of $H_{CF}=2$ kOe are shown in Fig. 5. Note that at $T=5$ K the samples with the PIL had a significantly

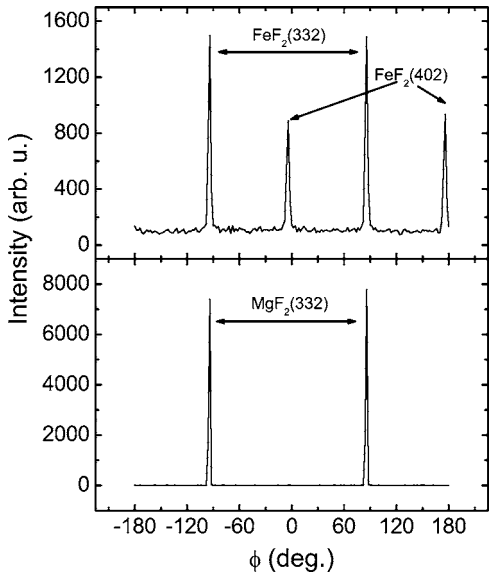

FIG. 4. ϕ scans of the MgF_2 and FeF_2 (332) peaks. The FeF_2 (402) lattice parameter is sufficiently similar to the (332) parameter that it is also visible.

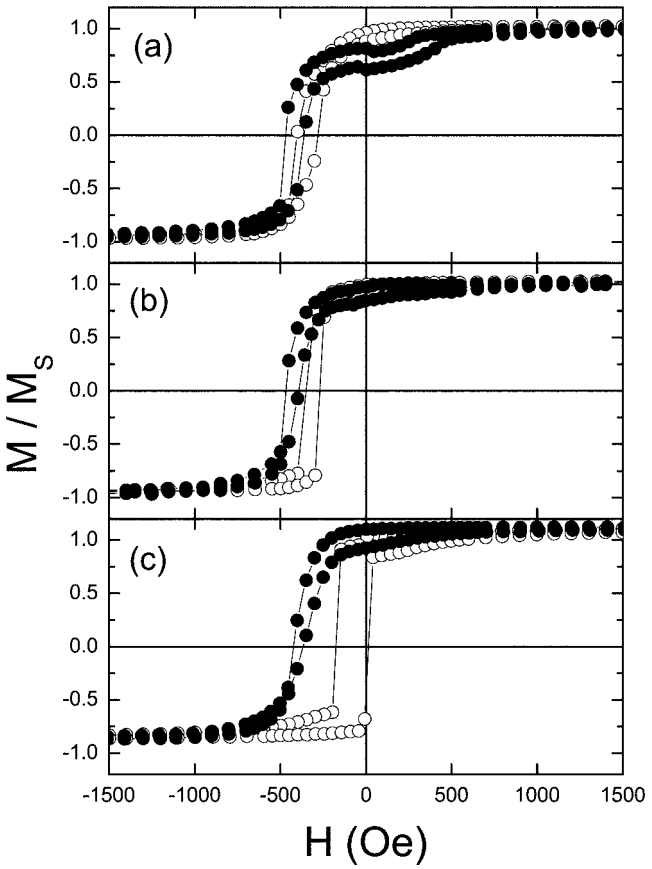

FIG. 5. Hysteresis loops measured at $T=5$ K for $x=$ (a) 0.97, (b) 0.77, and (c) 0.36 samples. Data for samples with a PIL (●) and without a PIL (○) are shown.

larger H_E. In addition, the coercivity was relatively small with respect to the exchange bias. The asymmetry in the hysteresis loops has been observed previously in transition metal fluorides and is believed to result from a fundamental asymmetry of the interface magnetic interaction.[16] The small part of the signal with $H_E>0$ for the PIL sample in Fig. 5(a) indicates that a small portion of the sample near the edge of the substrate had a slightly different interface interaction. This was verified by repeating this measurement after cooling in a smaller field of 500 Oe, since it is known that a positive H_E occurs when cooling in larger fields in samples with rougher interfaces.[14] In this case the loop only showed a negative H_E contribution. In any case, this problem does not affect the conclusions presented here. Figure 6 shows H_E and H_C as a function of temperature for all the samples in this study. For all samples H_E saturates at low temperatures (except for the $x=0.85$ sample) and H_C has a peak near the blocking temperature (T_B) above which $H_E=0$. Interestingly, the $x=0.85$ and 0.77 samples with the PIL show a change in sign of H_E at intermediate temperatures, as reported previously for a $x=0.82$ sample.[28] This is discussed in more detail below.

C. Dependence of T_B and H_E on x

In order to assess whether T_B and the Fe concentration x are correlated in a sensible way, in Fig. 7 we have plotted T_B as a function of x as was previously done for twinned samples.[13] The straight line in the plot is the expected relationship between T_N and x obtained from macroscopic single-crystal data for $x>0.25$.[29] Two important observations from these data are (1) the good agreement between the expected T_N and T_B (although some points are slightly below the line), and (2) the almost perfect agreement between the values of T_B for samples with and without the PIL for each value of x. This gives us confidence that the samples are ordering as they should and, because the PIL does not seem to change the T_B for the range of samples studied here, the onset of H_E is driven by the long-range AF order inside the bulk of the AF layer.

The interface exchange bias energy $\Delta E=H_E M t$, where M is the saturation magnetization of the ferromagnet (the standard value of 1400 emu/cm^3 for Co) and t is the thickness of the ferromagnetic layer determined from x-ray reflectivity, at $T=5$ K as a function of x, is shown in Fig. 8. Graphing ΔE instead of H_E normalizes all of the samples by taking care of small sample-dependent thickness variations in the F layer. For the samples with the PIL, ΔE does not vary much as a function of x, whereas for the samples without the PIL, ΔE decreases monotonically as x is decreased. In order to determine whether this decrease is due to an effective weakening of the interface exchange due to an increase in dilution, we have also plotted $\Delta E/x$ for the samples without the PIL in Fig. 8. For Fe-rich samples $\Delta E/x$ coincides well with the values of ΔE for the samples with the PIL. This indicates that the PIL had the desired effect of increasing the AF/F interface exchange to a level comparable to that of the pure sample. For the lower Fe concentration samples the PIL also increased the ordering within the AF because the $\Delta E/x$ data were lower than the ΔE data for the PIL samples. This is not unexpected because it was previously found that in twinned samples exchange bias was observed for samples with a PIL and $x=0$ at $T=5$ K,[13] indicating that the PIL can order independently of the underlying layer for low Fe.

D. Effects due to existence of critical concentration x_C

We now turn our attention to the samples that show a sign change in H_E as a function of temperature, previously observed on a $x=0.82$ sample.[28] Experiments were performed as a function of cooling field for all the samples. A sign change of H_E as a function of T was observed in the $x=0.77$ sample with PIL, although the switching temperature (T_S) is higher than for the $x=0.85$ sample, as shown in Fig. 6. Because neither lower nor higher Fe concentration samples displayed the effect, and because the structure of the $x=0.77$ and $x=0.85$ samples was not significantly different from the other samples, we conclude that the change in sign is a result of an instability of the AF magnetic structure that occurs in a finite, intermediate concentration range. This could be related to the critical concentration $x_C\sim 0.76$ in $Fe_xZn_{1-x}F_2$, above which AF domains are not expected to exist when the sample is field-cooled from above T_N because of a lack of percolation of magnetic impurities. This has been observed in both Monte Carlo simulations[30] and recent experimental data of bulk single crystals.[31] In this sense, the

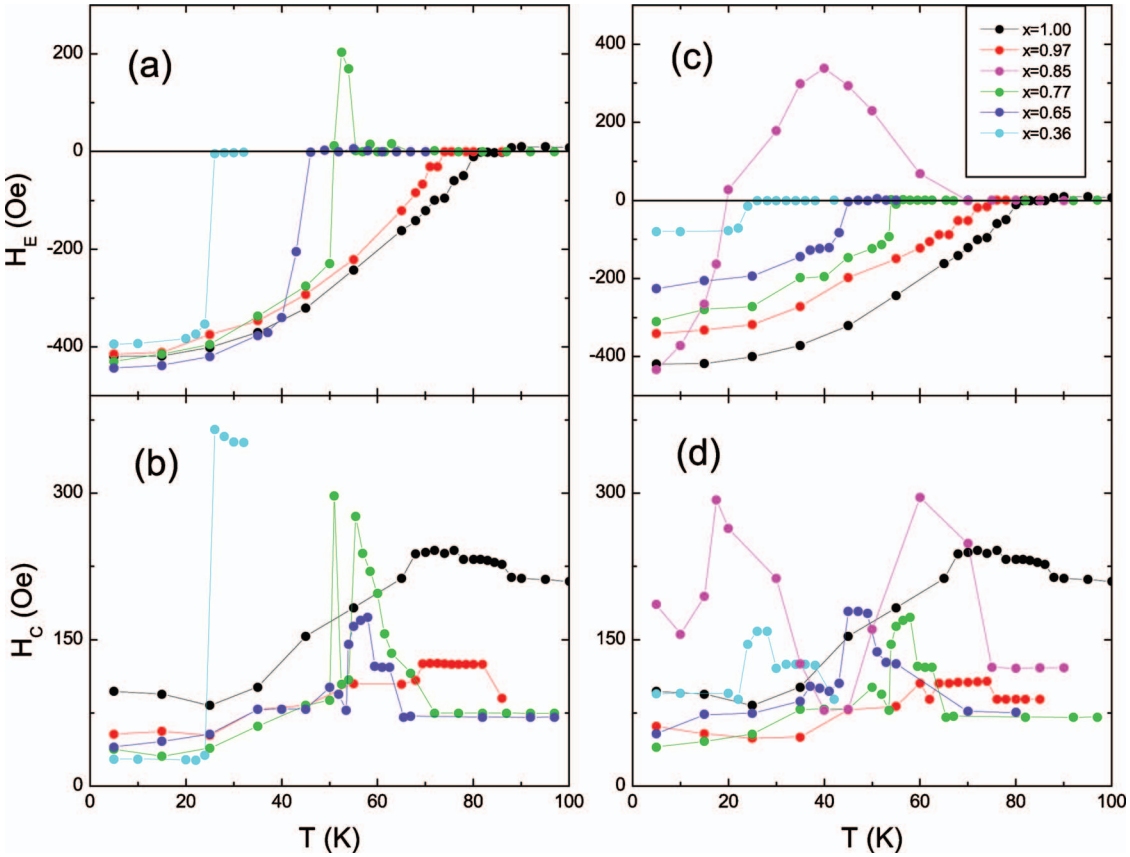

FIG. 6. (Color) Exchange bias (H_E) and coercivity (H_C) as a function of temperature for the samples used in this study. Data for samples with a PIL are shown in (a) and (b) while data for samples without a PIL are in (c) and (d). Legend shows the Fe concentration. Solid curves are guides to the eye.

PIL acts as a buffer between the F and the dilute AF, causing the AF to form a state that is in quasiequilibrium. As the temperature is increased and the field is reversed, the AF changes its configuration possibly by rotating all of the spins by 180°, thus reversing the sign of the exchange bias. Indeed, when the temperature was lowered from $T > T_S$ but with $T < T_B$ to $T = 5$ K, the sign of H_E remained positive.

We explored the role of the critical concentration further. If there is a critical concentration, we would expect the fro-

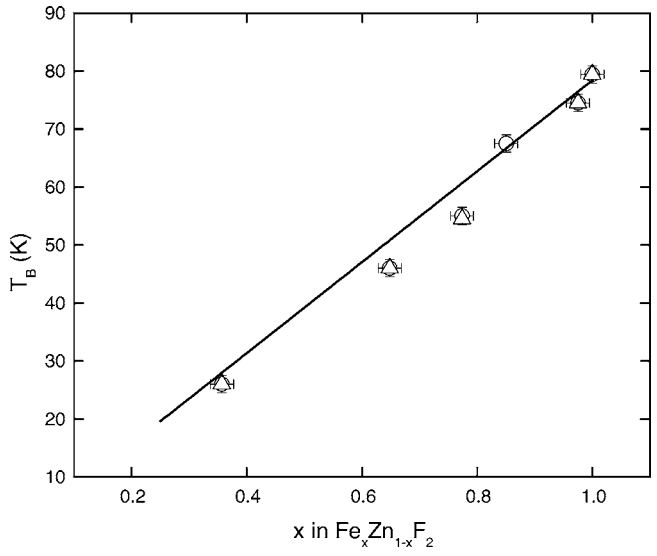

FIG. 7. Blocking temperature T_B as a function of Fe concentration x for samples with (◯) and without (△) the pure FeF_2 interface layer (PIL). The error bars in x come from the the uncertainty in the $Fe_xZn_{1-x}F_2$ (001) lattice parameter and the uncertainty in T_B from the step size in the temperature measurements (±1 K).

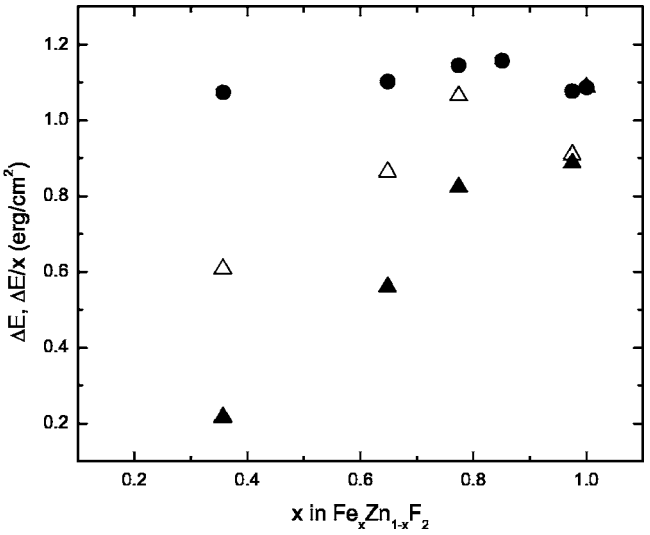

FIG. 8. Interface energy ΔE as a function of Fe concentration x for samples with (●) and without (▲) the pure FeF_2 interface layer (PIL). Also shown is $\Delta E/x$ (△) for the samples without the PIL.

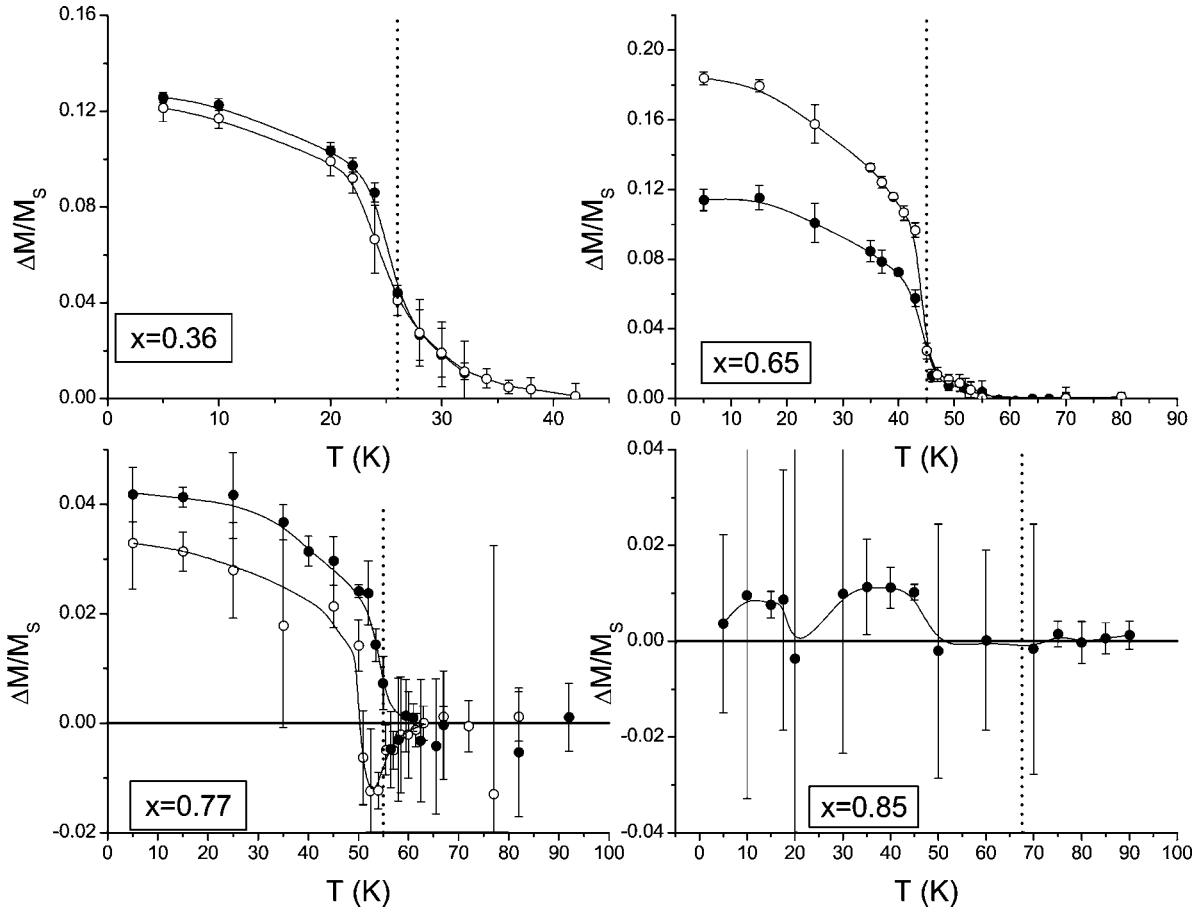

FIG. 9. Vertical shift of the hysteresis loops $\Delta M/M_S$ as a function of temperature for samples with the PIL (●) and without the PIL (○). Error bars are due to the standard deviation from averaging magnetization measurements near saturation. The dotted vertical lines indicate T_B. The solid curves are guides to the eye.

zen magnetic moment predicted by the domain-state model[11] to develop in the AF only for samples with $x<x_C$. To test this hypothesis, in Fig. 9 we have plotted the vertical shift of the hysteresis loops for samples with $x\leqslant 0.85$ as a function of temperature. Here, $\Delta M/M_S=(M(H_S+)-M(H_S-))/2M_S$, where $M(H_S\pm)$ is the magnetization at positive and negative saturation fields and M_S is the saturation magnetization. Notice that the shift is evident in the hysteresis loops plotted in Fig. 5. Clearly, there is a significant frozen magnetization generated for the samples for low Fe concentrations, and this shift tends to disappear at higher concentrations, in agreement with the hypothesis. An interesting point is that the frozen magnetization does not go to zero at T_B, and in fact T_B seems to coincide with the point of the maximum negative slope of the graph, at least for the $x=0.36$ and 0.65 samples. This indicates that the order in these samples is present at $T>T_B$, but the interface coupling is too weak to sustain exchange bias. This would explain why the points in Fig. 7 for $x<0.75$ are systematically below the expected single crysal T_N; in other words, $T_B<T_N$. Regarding the $x=0.75$ sample, there is a change of sign of $\Delta M/M_S$ that coincides with the change of sign of H_E shown in Fig. 6. This is an indication that the change in sign of H_E is due to a reversal of the domain structure in the antiferromagnet. The signal for the $x=0.85$ sample is too small to be measured accurately. The change in sign of H_E could be due to a change in the domain structure of the AF, perhaps a 180° rotation of the AF order parameter, due perhaps to the instability of the domain structure for $x\sim x_C$.

E. Comparison with previous work

Our experiments on single-crystalline $Fe_xZn_{1-x}F_2/Co$ bilayers demonstrate that there is at most a 10% enhanancement, near $x=0.85$, in the exchange bias as the Fe concentration is decreased from $x=1.0$ to 0.30. This result is at odds with measurements performed in $Co_xMg_{1-x}O/Co$ and twinned $Fe_xZn_{1-x}F_2/Co$ bilayers, as well as with theoretical expectations (domain state model). In the case of the twinned samples, an increase of approximately 30% was previously observed at intermediate values of x,[13] whereas in the CoO/Co case a significant increase of over 300% was measured.[10] At least for the $Fe_xZn_{1-x}F_2/Co$ system, this indicates that the previously-observed enhancement was related to structural defects in the twinned samples, which may permit some domain formation even for $x>x_C$. For the untwinned samples used in this study, we have clear evidence from the frozen magnetization data that the domains do form, but only at lower concentrations, in agreement with previous work. This indicates that the enhancement at larger

values of x is not possible because small domains do not form. For the $Co_xMg_{1-x}O/Co$ case, it is possible that because of its fcc structure, the critical concentration for domain formation is higher, thus permitting the formation of AF domains. This is possible because there are more nearest neighbors in the CoO structure and also because next-nearest-neighbor interactions are more important, all of which causes the percolation of the vacancies to occur at higher values of x. It also remains to be seen what is the role of structural defects in the $Co_xMg_{1-x}O$ system.

Finally, we note that a spontaneous magnetization was observed previously in a pure FeF_2 single crystal[32] and a dilute $Fe_{0.46}Zn_{0.54}F_2$ single crystal[33] when field cooled. In the case of the pure crystal, the authors suggested that the spontaneous magnetization was a result of a small piezomagnetic effect, which for a thin film would be very difficult to observe indeed. For the case of the dilute crystal, however, it is possible that part of the signal observed was due to the frozen moments similar to those observed in our thin film samples.

IV. CONCLUSIONS

We have measured the exchange bias properties of untwinned epitaxial $Fe_xZn_{1-x}F_2/Co$ bilayers as a function of x. We found an enhancement in the exchange bias of less than 10% with decreasing x, even though we were able to observe the frozen domains at low x required by the domain state model. We conclude that the lack of a large enhancement of the exchange bias as x is decreased is due to the fact that for $x > 0.76$ antiferromagnetic domains do not form very easily.

ACKNOWLEDGMENT

This work was supported by the U.S. National Science Foundation (Grant No. DMR-0400578).

*Present address: Department of Physics and Astronomy, Sonoma State University, Rohnert Park, CA 94928, USA.

[1] W. H. Meiklejohn and C. P. Bean, Phys. Rev. **102**, 1413 (1956).
[2] J. Nogués and I. K. Schuller, J. Magn. Magn. Mater. **192**, 203 (1999).
[3] A. E. Berkowitz and K. Takano, J. Magn. Magn. Mater. **200**, 552 (1999).
[4] W. H. Meiklejohn and C. P. Bean, Phys. Rev. **105**, 904 (1956).
[5] D. Mauri, H. C. Siegmann, and P. S. Bagus, J. Appl. Phys. **62**, 3047 (1987).
[6] A. P. Malozemoff, Phys. Rev. B **35**, 3679 (1987).
[7] A. P. Malozemoff, Phys. Rev. B **37**, 7673 (1988).
[8] A. P. Malozemoff, J. Appl. Phys. **63**, 3874 (1988).
[9] T. C. Schulthess and W. H. Butler, Phys. Rev. Lett. **81**, 4516 (1998).
[10] P. Miltényi, M. Gierlings, J. Keller, B. Beschoten, G. Guntherodt, U. Nowak, and K. D. Usadel, Phys. Rev. Lett. **84**, 4224 (2000).
[11] U. Nowak, K. D. Usadel, J. Keller, P. Miltényi, B. Beschoten, and G. Guntherodt, Phys. Rev. B **66**, 014430 (2002).
[12] J. Keller, P. Miltényi, B. Beschoten, G. Guntherodt, U. Nowak, and K. D. Usadel, Phys. Rev. B **66**, 014431 (2002).
[13] H. Shi, D. Lederman, and E. E. Fullerton, J. Appl. Phys. **91**, 7763 (2002).
[14] J. Nogués, D. Lederman, T. J. Moran, and I. K. Schuller, Phys. Rev. Lett. **76**, 4624 (1996).
[15] J. Nogués, D. Lederman, and I. K. Schuller, Appl. Phys. Lett. **68**, 3186 (1996).
[16] M. R. Fitzsimmons, P. Yashar, C. Leighton, I. K. Schuller, J. Nogués, C. F. Majkrzak, and J. A. Dura, Phys. Rev. Lett. **84**, 3986 (2000).
[17] M. Kiwi, J. Mejía-López, R. D. Portugal, and R. Ramírez, Europhys. Lett. **48**, 573 (1999).
[18] M. Kiwi, J. Mejía-López, R. D. Portugal, and R. Ramírez, Appl. Phys. Lett. **75**, 3995 (1999).
[19] M. Weissmann, A. M. Llois, and M. Kiwi, J. Magn. Magn. Mater. **234**, 19 (2001).
[20] I. N. Krivorotov, C. Leighton, J. Nogues, I. K. Schuller, and E. D. Dahlberg, Phys. Rev. B **68**, 054430 (2003).
[21] D. Lederman, R. Ramírez, and M. Kiwi, Phys. Rev. B **70**, 184422 (2004).
[22] H. Shi and D. Lederman, Phys. Rev. B **66**, 094426 (2002).
[23] M. Grimsditch, A. Hoffmann, P. Vavassori, H. Shi, and D. Lederman, Phys. Rev. Lett. **90**, 257201 (2003).
[24] J. McChesney, M. Hetzer, H. Shi, T. Charlton, and D. Lederman, J. Mater. Res. **16**, 1769 (2001).
[25] J. Nogués, T. J. Moran, D. Lederman, I. K. Schuller, and K. V. Rao, Phys. Rev. B **59**, 6984 (1999).
[26] B. Vidal and P. Vincent, Appl. Opt. **23**, 1794 (1984).
[27] B. E. Warren, *X-Ray Diffraction* (Dover Publications, New York, 1990), p. 253.
[28] H. Shi, D. Lederman, N. R. Dilley, R. C. Black, J. Diedrichs, K. Jensen, and M. B. Simmonds, J. Appl. Phys. **93**, 8600 (2003).
[29] G. K. Wertheim, D. N. E. Buchanan, and H. J. Guggenheim, Phys. Rev. **152**, 527 (1966).
[30] W. C. Barber and D. P. Belanger, J. Appl. Phys. **87**, 7049 (2000).
[31] W. C. Barber, F. Ye, D. P. Belanger, and J. A. Fernandez-Baca, Phys. Rev. B **69**, 024409 (2004).
[32] J. Mattsson, C. Djurberg, and P. Nordblad, J. Magn. Magn. Mater. **136**, L23 (1994).
[33] M. Lederman, J. Hammann, and R. Orbach, J. Phys.: Condens. Matter **165-166**, 165 (1990).